*Article*

# Formation of Stable Lithium-Containing Ceramics Using Solid-Phase Synthesis Method

**Dmitriy I. Shlimas** [1,2], **Artem L. Kozlovskiy** [1,2,*] and **Maxim V. Zdorovets** [1,2,3]

1    Engineering Profile Laboratory, L.N. Gumilyov Eurasian National University, Nur-Sultan 010008, Kazakhstan; Shlimas@mail.ru (D.I.S.); mzdorovets@gmail.com (M.V.Z.)
2    Laboratory of Solid State Physics, The Institute of Nuclear Physics of Republic of Kazakhstan, Almaty 050032, Kazakhstan
3    Department of Intelligent Information Technologies, Ural Federal University, 620075 Yekaterinburg, Russia
*    Correspondence: kozlovskiy.a@inp.kz

**Abstract:** Today, one of the most promising materials for a wide range of practical applications is lithium-containing ceramics based on $Li_2TiO_3$. At the same time, despite the high potential of their practical application, a number of questions remains related to the methods of their preparation, as well as the formation of a stable crystal structure and a pure-phase composition. To solve these issues, this paper proposes a method for obtaining stable $Li_2TiO_3$ ceramics, which is based on solid-phase synthesis combined with the high-temperature sintering of ceramics. During the studies carried out using X-ray diffraction methods, temperature dependences of phase transformations of the $TiO_2/Li_2Ti_6O_{13} \rightarrow Li_2TiO_3$ type were determined, according to which, at temperatures above 800 °C, the formation of a stable $Li_2TiO_3$ phase characterized by a high structural ordering degree of 89–91% is observed. The dependence of changes in structural, optical and ferroelectric characteristics on the conditions of synthesis and phase composition of ceramics was also determined.

**Keywords:** phase transformations; lithium-containing ceramics; blanket materials; $Li_2TiO_3$; crystallinity

## 1. Introduction

Lithium-containing ceramics such as $Li_2TiO_3$, $LiAlO_2$, $Li_2ZrO_3$, $Li_4SiO_4$ due to their unique physicochemical properties, as well as high resistance to chemical corrosion and mechanical stress, are widely used not only as a basis for ferroelectric devices, but also as materials for tritium propagation in thermonuclear power [1–5]. Great interest in these types of ceramics, in particular methods of their production, is due to the high yield of tritium, as well as the ability to control the morphological and structural features of ceramics [6,7]. At the same time, in recent years, most of the research related to these types of ceramics has been focused on a detailed study of the methods of their production, as well as control over the stability of properties, the possibility of varying the morphology and grain size, maintaining stability during production and further operation [8–10].

As is known, in most obtaining methods based on the processes of hydrothermal synthesis, the formation of stable phases in ceramics is difficult due to the large number of vacancy defects and structural distortions [11–15]. At the same time, in most cases, two-phase structures are obtained, the structure of which can be unstable.

Earlier, our research group proposed methods for the preparation of lithium-containing ceramics using a solid-phase synthesis method [16,17], which allows one to control with high accuracy not only morphological and structural parameters, but also to control the phase composition by varying the composition of salts, as well as the conditions of subsequent sintering. At the same time, both in the case of this method and in a number of other works, little attention is paid to the transition states of ceramics, which can have a significant effect on the further evolution of structural properties [18–20].

The aim of this work is to study phase transformations and the subsequent formation of a stable-phase composition of lithium-containing ceramics obtained using the method of solid-phase high-temperature synthesis. The relevance of this study is in the search for new methods of obtaining lithium-containing ceramics with high resistance and stability, which can later be used as a basis for blanket materials, as well as anode materials or ferroelectric devices.

## 2. Experimental Part

As the main method for obtaining ceramics, solid-phase synthesis combined with thermal annealing in a wide temperature range from 400 to 1000 °C was used. Before thermal annealing, initial mixtures of $TiO_2$ and $LiClO_4 \cdot 3H_2O$ powders, manufactured by Sigma Aldrich (Saint Louis, MI, USA), in a given stoichiometric ratio of 10:1 were subjected to intensive grinding in a planetary mill at a grinding speed of 400 rpm for 1 h. The annealing time was 5 h for each selected temperature, followed by cooling of the samples in a muffle furnace for 24 h until complete cooling and reaching room temperature. After annealing and cooling, the samples were placed in sealed containers for further research in order to avoid oxidation.

The study of morphological features was carried out using the scanning electron microscopy, implemented on the JEOL JEM—1400 Plus, JEOL, Japan microscope.

The phase composition, as well as the dynamics of changes in the structural parameters characterizing the structural changes occurring as a result of thermal annealing and phase transformation processes, was determined using the X-ray diffraction method. The studied X-ray diffraction patterns were obtained on a D8 Advance ECO powder X-ray diffractometer, Bruker. X-ray diffraction pattern recording conditions: Bragg–Brentano geometry in the angular range of $2\theta = 20$–$90°$, with a step of $0.03°$ and a spectrum acquisition time of 1 sec at a point. To determine the phases, the PDF-2(2016) database was used; phase refinement was carried out by comparative analysis of the position and intensities of diffraction reflexes of the obtained experimental values and card data from the database. The choice of the phase was based on the probability of coincidence of the reference values with the experimental data at the probability of coincidence of 85–90%. The phase selection also took into account the presence of structural distortions of the crystal lattice and interplanar distances, which lead to a shift and asymmetry of diffraction reflections.

Determination of the contribution of each phase was estimated using Equation (1):

$$V_{admixture} = \frac{RI_{phase}}{I_{admixture} + RI_{phase}} \tag{1}$$

where $I_{phase}$—average integrated intensity of the main phase of the diffraction line, $I_{admixture}$—the average integrated intensity of the additional phase, $R$ is the structural coefficient equal to 1.45.

The parameters were refined using the DiffracEVA v.4.2 program code, which is based on a full-profile analysis of the diffraction reflection assessment.

The degree of crystallinity was estimated by calculating the contributions of the areas of diffraction reflections and amorphous inclusions using the pseudo-Voigt functions. The analysis was carried out in the program code DiffracEVA v.4.2.

The density of ceramics depending on the annealing temperature was estimated by calculating changes in the volume of the crystal lattice and calculating the density according to the Formula (2):

$$p = \frac{1.6602 \sum AZ}{V_0} \tag{2}$$

where $V_0$—unit cell volume, $Z$ is the number of atoms in a crystal cell, $A$ is the atomic weight of atoms. The integral porosity of the samples under study was found according to the Formula (3):

$$P_{dil} = (1 - \frac{p}{p_0}) * 100\% \tag{3}$$

where $p_0$—reference density.

Determination of optical properties was carried out by recording and further analysis of UV-Vis transmission spectra obtained on a Jena Specord-250 BU spectrophotometer.

The ferroelectric characteristics were determined using a HIOKI IM 3570 Impedance Analyzer in a temperature range from 20 to 200 °C at a frequency of 10,000 Hz.

## 3. Results and Discussion

Figure 1 shows SEM images of the studied ceramics obtained after mechanochemical grinding and after thermal annealing at different sintering temperatures.
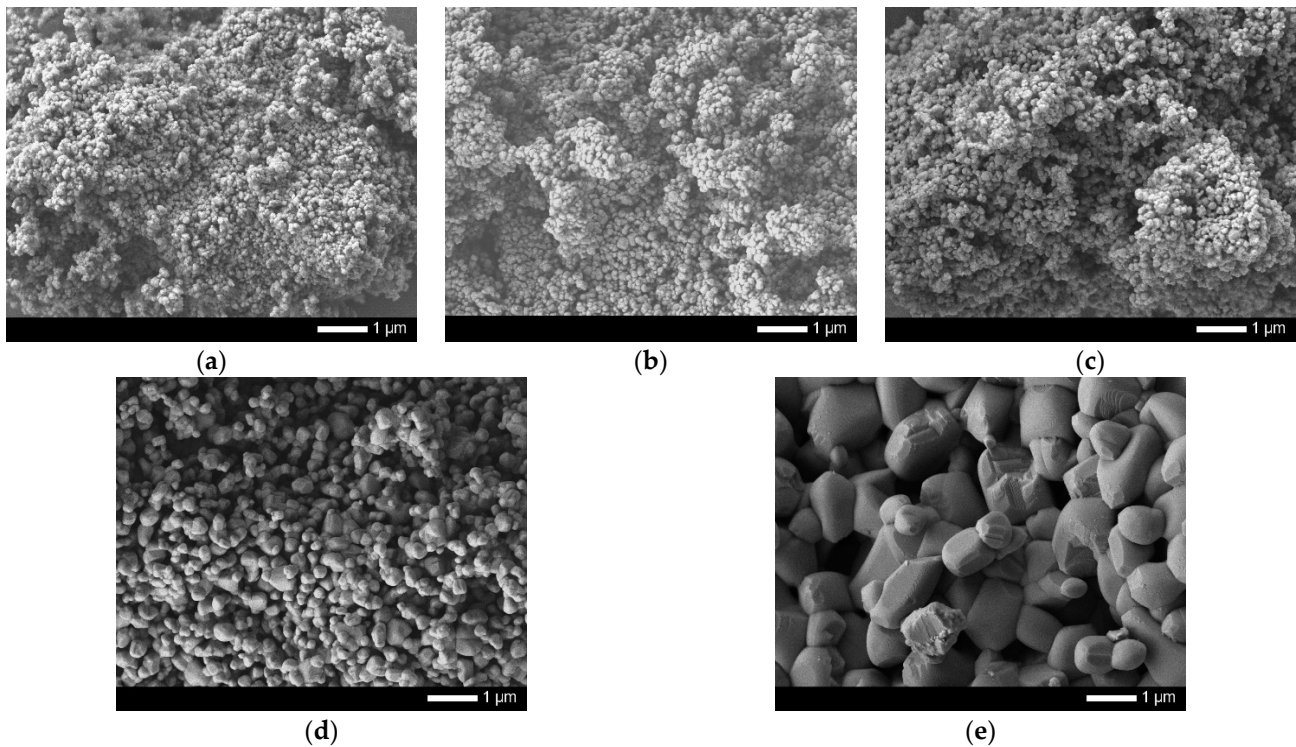


**Figure 1.** SEM images of synthesized ceramics: (**a**) pristine; (**b**) 400 °C; (**c**) 600 °C; (**d**) 800 °C; (**e**) 1000 °C.

The general trend of changes in grain morphology is as follows. In the initial state and at annealing temperatures of 400–600 °C, the grains are small spherical particles, the size of which does not exceed hundreds of nanometers. Moreover, these spherical particles are covered with smaller grains. An increase in the annealing temperature to 800 °C leads to an increase in the particle size up to several hundred nanometers, while they form fused agglomerates consisting of 5–10 particles. An increase in the annealing temperature to 1000 °C leads to the formation of large grains whose transverse dimensions exceed 1–2 μm. It can be seen that such an increase in grain size leads to a decrease in the number of grain boundaries and, consequently, the porosity of ceramics. Such changes indicate that with an increase in the annealing temperature, the main processes affecting the change in grain morphology are the processes of thermal fusion and enlargement of grains due to their fusion. These changes can also be accompanied by a change in the phase composition of grains, since sintering processes imply a rearrangement of the crystal structure.

Figure 2 shows the results of changes in phase composition of the studied ceramics depending on the annealing temperature, obtained on the basis of X-ray diffraction patterns. The general view of presented diffraction patterns indicates a change in the phase composition caused by the appearance of new diffraction reflections in the diffractograms obtained at different annealing temperatures. Additionally, a change in the reflections shape indicates a change in the structural ordering degree and a decrease in the concentration of the defective fraction in the structure of ceramics. As is known, the application of the

method of mechanochemical grinding of initial salts is based on the processes of crushing and subsequent formation of new compounds. Moreover, in most cases, the formation of such phases is accompanied by a large number of structural distortions and deformations resulting from the breaking of chemical and crystalline bonds. In this connection, the diffraction patterns of the samples after mechanochemical grinding are characterized by the presence of low-intensity peaks, asymmetric shapes, as well as large broadening, which characterizes structural distortions and deformations. During analysis of the initial samples diffraction patterns using the full-profile analysis method, it was found that diffraction reflections observed belong to different phases, which, according to the refinement of the PDF-2(2016) database, correspond to the tetragonal phase of $TiO_2$ and the monoclinic phase of $Li_2Ti_6O_{13}$. The presence of two phases, including the $Li_2Ti_6O_{13}$ phase after grinding, indicates phase formation processes initiation during mechanochemical grinding. In this case, the main phase in the initial state is the titanium dioxide phase, the content of which is more than 84%. The crystallinity degree, which characterizes structural perfection of the crystal lattice, for samples after mechanochemical grinding is not more than 70%. The presence of 30% amorphous-like disordered regions indicates that when milled, most of the chemical and crystalline bonds break, and the new phases formed contain a large number of structural distortions.
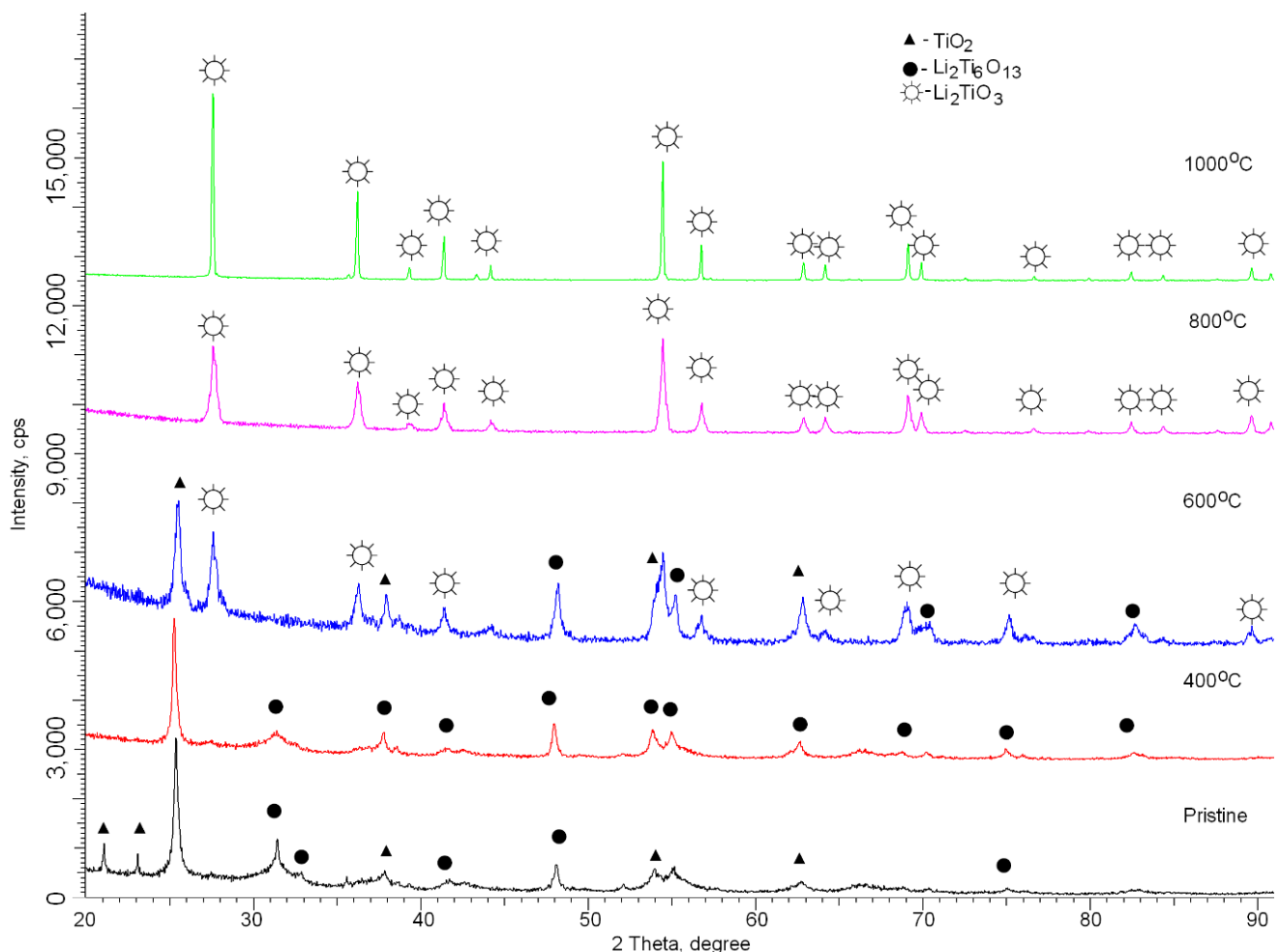


**Figure 2.** Results of X-ray diffraction of lithium-containing ceramics.

In the case of thermal annealing of the samples at a temperature of 400 °C, no new phases were observed, and all changes are associated only with a change in the shape of diffraction reflections, a decrease in their asymmetry, as well as a decrease in the contribution of disordering regions and a small increase in crystallinity degree to 73%. This

pattern of structural changes is due to a low ordering degree and a decrease in deformation contributions, which occur as a result of a change in the magnitude of atoms thermal vibrations and partial filling of vacancy defects in the crystal lattice structure. At the same time, an insignificant increase in the contribution of the $Li_2Ti_6O_{13}$ phase to the structure of ceramics is also observed, which is due to the processes of phase transformations and orderings.

A different picture is observed for ceramic samples annealed at 600 °C, at which a new family of diffraction reflections characteristic of the monoclinic $Li_2TiO_3$ phase appears. The appearance of this phase is associated with the phase transformation processes $Li_2Ti_6O_{13} \rightarrow Li_2TiO_3$ and the partial transformation of the $TiO_2$ phase by replacing titanium atoms with lithium atoms, followed by rearrangement into the $Li_2TiO_3$ phase. In this case, the strongly asymmetric shape of the diffraction reflections for all observed phases indicates large deformation processes that are associated with the processes of substitution and implantation.

Figure 3a shows the results of changes in phase composition of the studied ceramics depending on the annealing temperature, according to which completion of phase transformations of the $TiO_2/Li_2Ti_6O_{13} \rightarrow Li_2TiO_3$ type is observed at annealing temperatures of 800–1000 °C. At the same time, an increase in the annealing temperature above 600 °C leads to a complete displacement of $TiO_2$ and $Li_2Ti_6O_{13}$ phases and the formation of the $Li_2TiO_3$ phase. An increase in annealing temperature to 1000 °C leads to an increase in structural ordering, characterized by an increase in the intensity of diffraction reflections and a decrease in reflections asymmetry degree, as well as an increase in the size of crystallites and an almost complete decrease in deformation contributions to the structure (see data in Figure 3b). The deformation contributions were estimated by comparative analysis of the diffraction maxima positions and the corresponding interplanar distances with similar values of interplanar distances for the reference samples. Additionally, from the data in Figure 3b, which reflects changes in the crystallinity degree, it can be seen that samples annealed at a temperature of 800–1000 °C are observed to increase the crystallinity degree by 5–7% compared to the samples annealed at a temperature of 600 °C and by 20–22% compared with the initial samples. This pattern of change in the crystallinity degree indicates a decrease in amorphous or disordered regions due to the thermal annealing and the phase change processes initiated by it, followed by the formation of a stable monoclinic $Li_2TiO_3$ phase.
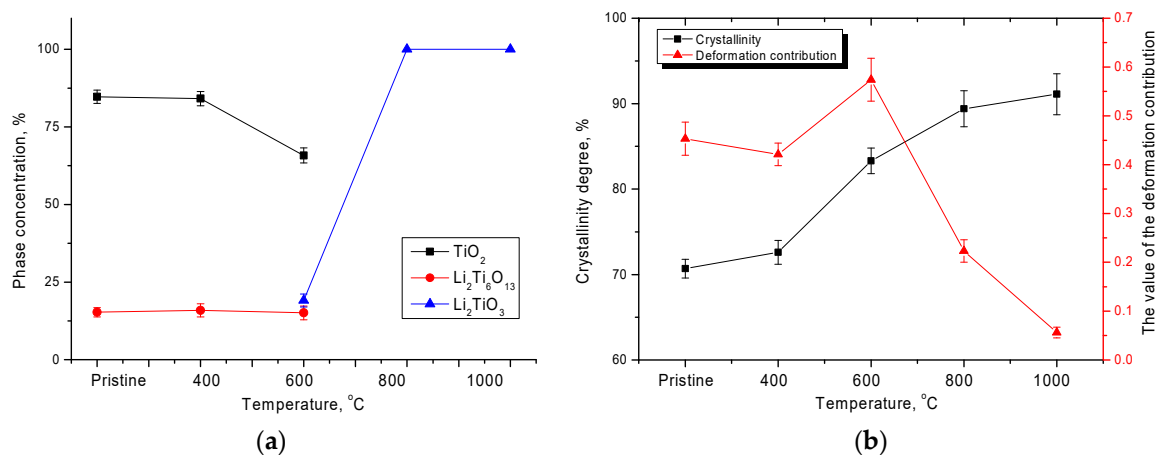


**Figure 3.** (**a**) Diagram of ceramic phase composition depending on annealing temperature; (**b**) graph of changes in the crystallinity degree and deformation contributions to the change in the shape of diffraction reflections.

Table 1 shows the results of changing crystal lattice parameters for all established phases depending on the annealing temperature. The parameters were determined according to the standard method for refining the parameters in the DiffracEVA v.4.2 program

code, based on refining the angular position of the diffraction maxima and the corresponding positions of the interplanar distances, followed by recalculation using the Nelson–Taylor equations. From the data presented, it can be seen that the formation of the third phase of $Li_2TiO_3$ leads to an increase in parameters distortion, as is also evidenced by a sharp increase in deformation contributions presented in Figure 3b. However, subsequent displacement of $TiO_2$ and $Li_2Ti_6O_{13}$ phases leads to structural ordering and a decrease in deformation contributions.

**Table 1.** Crystallographic characteristics of the studied ceramics.

| Phase | Pristine | 400 °C | 600 °C | 800 °C | 1000 °C |
|---|---|---|---|---|---|
| $TiO_2$—Tetragonal I-41/amd(141) | a = 3.76848 Å, c = 9.49348 Å, V = 134.46 Å3 | a = 3.78045 Å, c = 9.52512 Å, V = 136.13 Å3 | a = 3.79081 Å, c = 9.50084 Å, V = 137.09 Å3 | - | - |
| $Li_2Ti_6O_{13}$ Monoclinic C2/m(12) | a = 15.37553 Å, b = 3.73343 Å, c = 9.18879 Å, β = 99.282°, V = 520.56 Å3 | a = 15.35443 Å, b = 3.74880 Å, c = 9.16537 Å, β = 99.651°, V = 520.10 Å3 | a = 15.36529 Å, b = 3.78630 Å, c = 9.14920 Å, β = 99.593°, V = 524.23 Å3 | - | - |
| $Li_2TiO_3$ Monoclinic C2/c(15) | - | - | a = 5.04146 Å, b = 8.74452 Å, c = 9.72461 Å, β = 99.917°, V = 422.30 Å3 | a = 5.03849 Å, b = 8.73595 Å, c = 9.77228 Å, β = 99.623°, V = 424.08 Å3 | a = 5.05431 Å, b = 8.72909 Å, c = 9.69982 Å, β = 99.741°, V = 421.78 Å3 |

Figure 4 shows the results of changes in ceramics density and their porosity depending on the annealing temperature. At the initial stage, in the initial state and annealed at a temperature of 400 °C, the density of ceramics is more than 3.8 g/cm$^3$, which is due to the dominance of the $TiO_2$ phase, the density of which is much higher than the density of the $Li_2Ti_6O_{13}$ phase (3.89 g/cm$^3$ vs. 3.27 g/cm$^3$). At the same time, for both samples, a high percentage of ceramics porosity is observed, which is due to a low structural ordering degree and large structural deformations. An increase in the annealing temperature to 600 °C leading to the appearance of the third phase of $Li_2TiO_3$ leads to a decrease in the density, which is due to the displacement of the $TiO_2$ phase and a decrease in its concentration. At the same time, the formation of a three-phase structure also leads to a decrease in ceramics porosity. At temperatures of 800–1000 °C, ceramics density is caused only by structural changes in the $Li_2TiO_3$ phase and its structural orderings, which lead to an increase in density and a decrease in porosity to 0.6%.
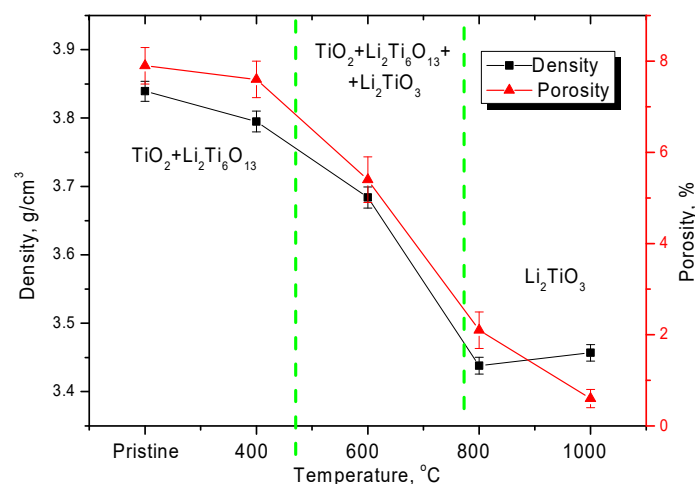


**Figure 4.** Graph of changes in density and porosity of ceramics depending on annealing temperature.

The optical properties of the synthesized ceramics were studied using the UV-Vis spectroscopy method by obtaining and further analyzing the transmission spectra in the wavelength range from 350 to 1000 nm. The general view of the obtained spectra presented in Figure 5 is characterized by the presence of a fundamental absorption edge in the region of 360–400 nm (the border of the UV region and visible light), as well as a transmission value in the range of 75–90% in the region of visible light and near-IR. An increase in the annealing temperature and, consequently, as shown by the results of X-ray phase analysis, leading to a change in the phase composition of ceramics, leads to a shift in the fundamental absorption edge, as well as to a change in the transmission value. It should be noted that for the samples obtained at an annealing temperature of 800–1000 °C, an additional wide absorption band appears in the region of 600–680 nm, the formation of which is associated with the $Li_2TiO_3$ phase and a change in the electron density in ceramics.
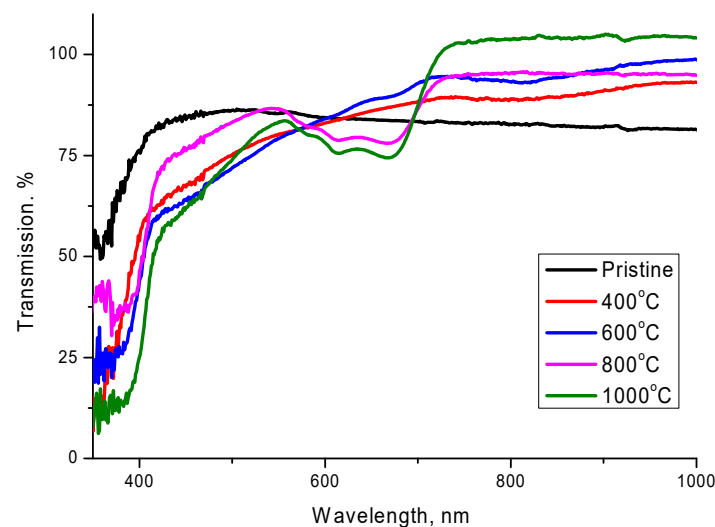


**Figure 5.** UV-Vis transmission spectra of synthesized ceramics depending on the change in annealing temperature.

Figure 6 shows the results of the change in the dielectric constant and the change in the Curie–Weiss temperature. The general view of the changes can be divided into two stages, which are characteristic of different types of phase transitions. In the case of ceramics in the initial state and annealed at a temperature of 400 °C, a smooth change in the dielectric constant from temperature up to reaching a maximum in the region of 135–145 °C indicates a second-order phase transition. At the same time, the maximum value of the dielectric constant does not exceed 4200–4800. This behavior of changes in the dielectric constant, as well as the values of the Curie–Weiss temperature, which amounted to 143.7 °C and 137.4 °C for the samples in the initial and annealed at 400 °C, respectively, is primarily due to the presence in the structure of a high content of the titanium dioxide phase, as well as the metastable $Li_2Ti_6O_{13}$ phase.

At a temperature of 600 °C and above, the temperature dependence of the change in the dielectric constant is characteristic of first-order phase transitions, which are characterized by a sharp rise in the value of the dielectric constant near the Curie temperature and a smooth decrease after passing the maximum, which indicates the relaxor nature of the change in the properties of ferroelectrics. Additionally, in this case, a significant change in the Curie–Weiss temperature is observed, which indicates a change in the nature of phase transitions and their type. This behavior is primarily associated with a change in the phase composition and further dominance of the stable $Li_2TiO_3$ phase in the structure, as well as a decrease in porosity and a change in the density of ceramics. The formation of a stable $Li_2TiO_3$ phase also leads to an increase in the maximum of the dielectric constant and the value of spontaneous polarization, the result of which is shown in Figure 7a.
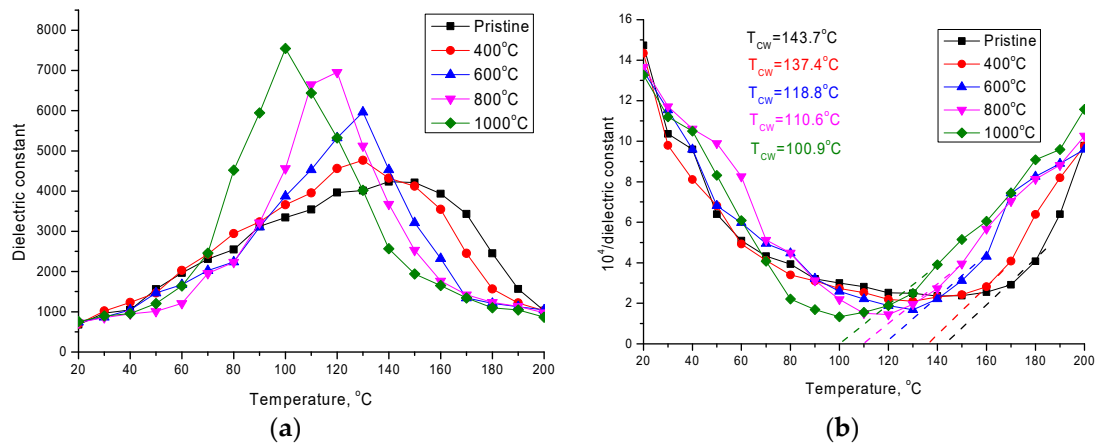
**Figure 6.** (**a**) Graph of changes in the dielectric constant; (**b**) graph of inverse dielectric constant and Curie–Weiss temperature.
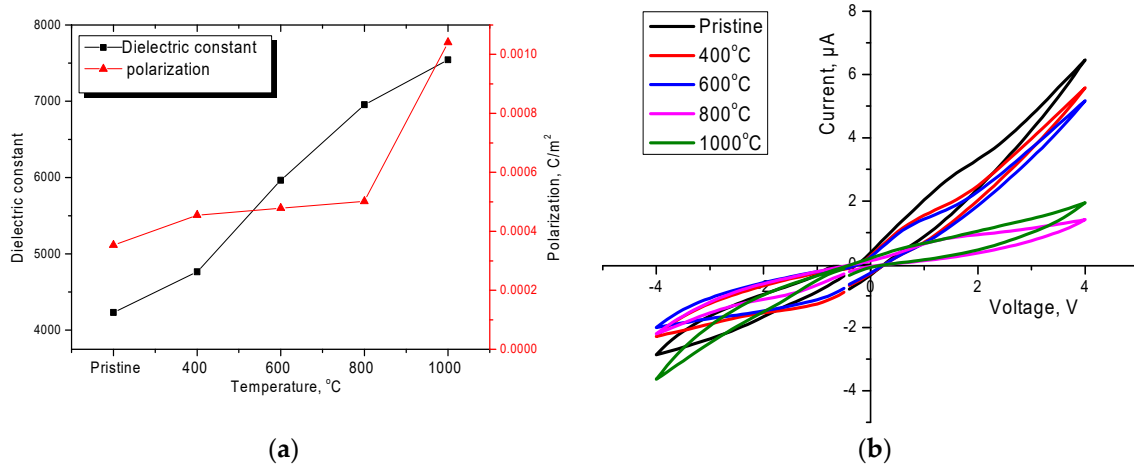


**Figure 7.** (**a**) Graph of the change in the dielectric constant maximum and spontaneous polarization; (**b**) graphs of cyclic volt-ampere characteristics of ceramics.

Figure 7b shows the graphs of the cyclic I–V curves of the studied ceramics depending on the annealing conditions. As can be seen from the above, an increase in the annealing temperature, leading to structural ordering and a change in the phase composition, leads to a decrease in the width of the hysteresis loops, as well as an increase in resistance.

## 4. Conclusions

This paper presents the results of changes in the morphological, structural, optical and ferroelectric properties of lithium-containing ceramics depending on the annealing temperature. Scanning electron microscopy, X-ray diffraction, optical and impedance spectroscopy were used as research methods. As a result of the studies carried out, it was found that an increase in the annealing temperature leads to an increase in the grain size at a temperature of 1000 °C and a decrease in ceramics porosity. Based on the obtained X-ray data, the temperature dependence of the change in ceramics phase composition was established and a diagram of phase transformations was plotted, the final stage of which is the formation of a stable $Li_2TiO_3$ phase with a high structural ordering degree and small values of deformation contributions. During the determination of ferroelectric characteristics, it was found that the formation of a stable $Li_2TiO_3$ phase leads to an increase in dielectric constant, as well as a decrease in the Curie–Weiss temperature.

# References

1. Zhou, Q.; Togari, A.; Nakata, M.; Zhao, M.; Sun, F.; Xu, Q.; Oya, Y. Release kinetics of tritium generation in neutron irradiated biphasic $Li_2TiO_3$–$Li_4SiO_4$ ceramic breeder. *J. Nucl.* **2019**, *522*, 286–293. [CrossRef]
2. Jung, C.H.; Lee, S.J.; Kriven, W.M.; Park, J.Y.; Ryu, W.S. A polymer solution technique for the synthesis of nano-sized $Li_2TiO_3$ ceramic breeder powders. *J. Nucl. Mater.* **2008**, *373*, 194–198. [CrossRef]
3. Wang, H.; Yang, M.; Gong, Y.; Feng, L.; Dang, C.; Shi, Y.; Shi, Q.; Wei, J.; Liao, Z.; Lu, T. Fabrication of nanostructured $Li_2TiO_3$ ceramic pebbles as tritium breeders using powder particles synthesised via a CTAB-assisted method. *Ceram. Int.* **2017**, *43*, 5680–5686. [CrossRef]
4. Zhou, Q.; Xue, L.; Wang, Y.; Li, H.; Chikada, T.; Oya, Y.; Yan, Y. Preparation of $Li_2TiO_3$ ceramic with nano-sized pores by ultrasonic-assisted solution combustion. *J. Eur. Ceram. Soc.* **2017**, *37*, 3595–3602. [CrossRef]
5. Xu, C.; Li, Y.; Li, L.; Wang, X.; Han, Q.; Ren, M.; Ye, W. Effect of $Cl^-$ on the properties of $Li_2TiO_3$ ceramic powders synthesized by in-situ hydrolysis. *Ceram. Int.* **2014**, *40*, 7213–7218. [CrossRef]
6. Min, K.M.; Park, Y.H.; Cho, S. Synthesis of $Li_2TiO_3$ powder with high crystalline structure for tritium breeding material by ion-exchange process. *Fusion Eng. Des.* **2016**, *109*, 326–329. [CrossRef]
7. Kolb, M.H.H.; Mukai, K.; Knitter, R.; Hoshino, T. Li4SiO4 based breeder ceramics with $Li_2TiO_3$, $LiAlO_2$ and LiXLaYTiO3 additions, part I: Fabrication. *Fusion Eng. Des.* **2017**, *115*, 39–48. [CrossRef]
8. Rao, G.J.; Mazumder, R.; Bhattacharyya, S.; Chaudhuri, P. Fabrication and characterization of $Li_4SiO_4$-$Li_2TiO_3$ composite ceramic pebbles using extrusion and spherodization technique. *J. Eur. Ceram. Soc.* **2018**, *38*, 5174–5183.
9. Yang, M.; Wang, H.; Chen, R.; Gong, Y.; Huang, Z.; Ran, G.; Chen, X.; Lu, T.; Xiao, C. Comparison of the microwave and conventional sintering of $Li_2TiO_3$ ceramic pebbles. *Ceram. Int.* **2018**, *44*, 19672–19677. [CrossRef]
10. Li, Y.; Xu, C.; Wang, X.; Li, L.; Kong, L. Synthesis of $Li_2TiO_3$ ceramic breeder powders by in-situ hydrolysis and its characterization. *Mater. Lett.* **2012**, *89*, 25–27. [CrossRef]
11. Jung, C.H. Sintering characterization of $Li_2TiO_3$ ceramic breeder powders prepared by the solution combustion synthesis process. *J. Nucl. Mater.* **2005**, *341*, 148–152. [CrossRef]
12. Yu, C.L.; Yanagisawa, K.; Kamiya, S.; Kozawa, T.; Ueda, T. Monoclinic $Li_2TiO_3$ nano-particles via hydrothermal reaction: Processing and structure. *Ceram. Int.* **2014**, *40*, 1901–1908. [CrossRef]
13. Guo, H.; Wang, H.; Chen, R.; Huang, Z.; Gong, Y.; Zeng, Y.; Jiang, Y.; Qi, J.; Shi, Q.; Lu, T. Low-cost fabrication of $Li_2TiO_3$ tritium breeding ceramic pebbles via low-temperature solid-state precursor method. *Ceram. Int.* **2019**, *45*, 17114–17119. [CrossRef]
14. Wang, H.; Guo, H.; Chen, R.; Zeng, Y.; Yang, M.; Gong, Y.; Shi, Y.; Ye, D.; Liao, Z.; Qi, J.; et al. A novel mass production method for $Li_2TiO_3$ tritium breeder ceramic pebbles using polyvinyl alcohol (PVA) and polyvinyl pyrrolidone (PVP) assisted granulation method. *Ceram. Int.* **2020**, *46*, 4167–4173. [CrossRef]
15. Shlimas, D.; Kozlovskiy, A.L.; Zdorovets, M. Study of Corrosion Resistance and Degradation Mechanisms in $LiTiO_2$-$Li_2TiO_3$ Ceramic. *Crystals* **2021**, *11*, 753. [CrossRef]
16. Shlimas, D.I.; Kozlovskiy, A.L.; Zdorovets, M.V. Study of the formation effect of the cubic phase of $LiTiO_2$ on the structural, optical, and mechanical properties of Li 2 ± x Ti 1 ± x O 3 ceramics with different contents of the X component. *J. Mater. Sci. Mater. Electron.* **2021**, *32*, 7410–7422. [CrossRef]
17. Kozlovskiy, A.L.; Kenzhina, I.E.; Zdorovets, M.V. Zdorovets. Study of radiation resistance to helium swelling of AlN ceramics in case of irradiation with low-energy He 2+ ions with energy of 40 keV. *J. Mater. Sci. Mater. Electron.* **2021**, *32*, 14347–14357. [CrossRef]

18. Kulsartov, T.; Kenzhina, I.; Tolenova, A.; Kenzhin, Y.; Shaimerdenov, A.; Nesterov, Y.; Gizatulin, S.; Chikhray, Y.; Gluchshenko, A. Modeling of hydrogen isotopes release from lithium ceramics $Li_2TiO_3$ during in-situ experiments using vacuum extraction method. *Fusion Eng. Des.* **2021**, *170*, 112705. [CrossRef]

19. Zeng, Y.; Chen, R.; Yang, M.; Wang, H.; Guo, H.; Shi, Y.; Huang, Z.; Qi, J.; Shi, Q.; Lu, T. Fast fabrication of high quality $Li_2TiO_3$–$Li_4SiO_4$ biphasic ceramic pebbles by microwave sintering: In comparison with conventional sintering. *Ceram. Int.* **2019**, *45*, 19022–19026. [CrossRef]

20. Zhumatayeva, I.Z.; Kenzhina, I.E.; Kozlovskiy, A.L.; Zdorovets, M.V. The study of the prospects for the use of Li0. 15Sr0. 85TiO$_3$ ceramics. *J. Mater. Sci. Mater. Electron.* **2020**, *31*, 6764–6772. [CrossRef]